Selective Reconstitution of Human D4 Dopamine Receptor Variants with $G_i\alpha$ Subtypes†

Manija A. Kazmi,[‡,§,||] Lenore A. Snyder,[§,||,⊥] Aaron M. Cypess,[§] Stephen G. Graber,[#] and Thomas P. Sakmar*[,‡,§]

Howard Hughes Medical Institute, Laboratory of Molecular Biology and Biochemistry, The Rockefeller University, New York, New York 10021, and Department of Pharmacology and Toxicology, West Virginia University, Morgantown, West Virginia 26506

Received October 11, 1999; Revised Manuscript Received December 23, 1999

ABSTRACT: G protein-coupled receptors (GPCRs) are seven-transmembrane (TM) helical proteins that bind extracellular molecules and transduce signals by coupling to heterotrimeric G proteins in the cytoplasm. The human D4 dopamine receptor is a particularly interesting GPCR because the polypeptide loop linking TM helices 5 and 6 (loop i3) may contain from 2 to 10 similar direct hexadecapeptide repeats. The precise role of loop i3 in D4 receptor function is not known. To clarify the role of loop i3 in G protein coupling, we constructed synthetic genes for the three main D4 receptor variants. D4-2, D4-4, and D4-7 receptors contain 2, 4, and 7 imperfect hexadecapeptide repeats in loop i3, respectively. We expressed and characterized the synthetic genes and found no significant effect of the D4 receptor polymorphisms on antagonist or agonist binding. We developed a cell-based assay where activated D4 receptors coupled to a Pertussis toxin-sensitive pathway to increase intracellular calcium concentration. Studies using receptor mutants showed that the regions of loop i3 near TM helices 5 and 6 were required for G protein coupling. The hexadecapeptide repeats were not required for G protein-mediated calcium flux. Cell membranes containing expressed D4 receptors and receptor mutants were reconstituted with purified recombinant G protein α subunits. The results show that each D4 receptor variant is capable of coupling to several $G_i\alpha$ subtypes. Furthermore, there is no evidence of any quantitative difference in G protein coupling related to the number of hexadecapeptide repeats in loop i3. Thus, loop i3 is required for D4 receptors to activate G proteins. However, the polymorphic region of the loop does not appear to affect the specificity or efficiency of $G_i\alpha$ coupling.

The G protein-coupled receptors (GPCRs)[1] make up a family of seven-helical transmembrane (TM) proteins found in virtually all tissues in vertebrates. They perform the critical physiological role of binding extracellular hormones and drugs and transducing signals into the cytoplasm. The hundreds of GPCRs make up approximately 1−2% of the total number of genes in the human genome (*1*), yet they typically couple to a much smaller set of cytoplasmic transducers, the heterotrimeric G proteins. These G proteins consist of a nucleotide-binding α subunit and a heterodimeric $\beta\gamma$ subunit, which associate to form a heterotrimer when α is bound to GDP. Hormone binding to receptor stabilizes its active conformation and induces the formation of a ternary complex with the G protein at the plasma membrane. The α subunit then exchanges GDP for cytoplasmic GTP, causing the heterotrimeric complex to split into a $\beta\gamma$ heterodimer and a GTP-bound α subunit (*2*). Depending on the cell type and the particular G protein, either α subunit, $\beta\gamma$ subunit, or both regulate downstream effector molecules that continue the intracellular signal transduction cascade.

A large number of polymorphic variants of the D4 dopamine receptor gene exist in the human population. The gene varies in the nucleotide sequence of the region encoding the intracellular polypeptide loop that links TM segments 5 and 6. This loop i3 may contain from 2 to 7 or more similar 48 base pair repeats (Figure 1). The different nucleotide repeats code for more than 18 different hexadecapeptide sequences. The role of loop i3 in receptor function is not known. However, loop i3 of the human D4 dopamine receptor contains pΦPpXp amino acid sequence motifs characteristic of SH3-binding domains at positions 241−246 and 246−251 (*3*, *4*) (Figure 1). Although a number of GPCRs, including the β1-adrenergic and m4-muscarinic receptors, contain a less specific PXXP motif in loop i3 or the carboxyl-terminal tail, the pΦPpXp sequence motif is unique to the D4 dopamine receptor. Oldenhof et al. showed various D4 dopamine receptors and expressed loop fragments

† This research was supported in part by Aaron Diamond Foundation Award HRI-817-5332, National Institutes of Health Grants CA09673 and DK54718, Medical Scientist Training Program Grant GM07739, and National Science Foundation Grant MCB9870839. This paper is dedicated to Dr. H. G. Khorana on the occasion of the "International Symposium on Nucleic Acids and Signal Transduction".

* To whom correspondence should be addressed at Box 284, Rockefeller University, 1230 York Ave., New York, NY 10021. Telephone: 212-327-8288, FAX: 212-327-7904, E-mail: sakmar@rockvax.rockefeller.edu.

‡ Howard Hughes Medical Institute.

§ The Rockefeller University.

|| These authors contributed equally.

⊥ Present address: Linguagen Corp., Clifton, NJ 07015.

West Virginia University.

[1] Abbreviations: bp, base pair(s); GPCR, G protein-coupled receptor; G_t, transducin; loop i3, third intracellular loop; PBS, phosphate-buffered saline; PTX, Pertussis toxin; TM, transmembrane.

10.1021/bi992354c CCC: $19.00
Published on Web 03/07/2000

bound weakly to some proteins containing SH3 domains including Nck and Grb2 (*3*). Certain deletions of the putative SH3-binding sites also affected receptor internalization. The results of immunofluorescence studies suggested that these receptors were constitutively internalized.

Intracellular loop i3 has also been shown to be involved in G protein coupling and specificity in virtually every GPCR studied, including members of both the Type I (rhodopsin-like) and Type II (glucagon receptor-like) receptor classes. The human D4 dopamine receptor has been shown to couple to the $G_i\alpha$ class of G proteins (*5*), which generally inhibits adenylyl cyclase to reduce intracellular cAMP levels. Under certain assay conditions, activation of D4 dopamine receptors can inhibit forskolin-stimulated adenylyl cyclase activity and (±)-Bay K 8644-induced ion flux by L-type Ca^{2+} channels. Generally, the physiological effects of D4 receptor activation are consistent with G_i coupling. However, the results of pharmacological characterization of G protein coupling of the D4 receptor in cell lines and transfected cells appear uncertain. No direct quantitative biochemical studies of G protein−receptor interaction have been carried out for the D4 dopamine receptor, and no reconstitution studies have been reported. In particular, the precise role of the loop i3 polymorphisms, if any, in G protein coupling efficiency and specificity has not been clearly defined.

To address this problem, we developed a heterologous expression system for synthetic genes encoding several D4 receptor variants and mutants. We characterized a PTX-sensitive signal transduction pathway that couples D4 receptor activation to intracellular calcium flux in HEK 293T cells. Finally, we reconstituted expressed receptors with purified recombinant $G_i\alpha$ subunits and directly measured quinpirole-stimulated GTPγS binding. We found that regions of loop i3 near the membrane borders of both TM helices 5 and 6 are required for G protein coupling as demonstrated in both cell-based calcium flux assays and reconstitution assays. Our results show that each D4 receptor variant is capable of coupling to several $G_i\alpha$ subtypes. Furthermore, there is no evidence of any quantitative difference in G protein coupling related to the number of hexadecapeptide repeats in loop i3.

EXPERIMENTAL PROCEDURES

Design and Synthesis of Genes Encoding the Major Variants of the Human D4 Dopamine Receptor. The nucleotide sequences of the synthetic genes for the human D4 dopamine receptor variants D4-2, D4-4, and D4-7 are available at the GenBank/EMBL Data Bank (accession numbers AF119328, AF119329, and AF119330, respectively). The design of the synthetic genes was carried out using strategies that have been described elsewhere (*6*−*8*). In short, the genes code for the native amino acid sequences but contain a large number of unique endonuclease restriction sites and a reduced G+C base content compared with the original nucleotide sequences. The Khorana method, in which both upper and lower strands are chemically synthesized, was employed to produce four fragments for the D4-7 gene, which was constructed first. The oligonucleotides were synthesized on an Applied Biosystems model 392 synthesizer and ranged in length from 50 to 90 bases. The gene fragments were PCR-amplified after T4 DNA ligase-catalyzed duplex joining reactions. Each fragment was cloned and sequenced independently in pGEM-2 (Promega). The four gene fragments were assembled into a full-length gene flanked by 5′-*Eco*RI and 3′-*Not*I restriction sites. The D4-2 gene was produced by excising a *Bsu*36I restriction fragment followed by re-ligation. The D4-4 gene was produced by replacing the 217 base pair (bp) *Rsr*II−*Ava*I restriction fragment of the D4-7 gene with a 71 bp synthetic duplex. The lengths of the D4-2, D4-4, and D4-7 synthetic genes are 1170, 1266, and 1410 bp, respectively. The three genes are identical except for the region corresponding to the cytoplasmic loop i3 as shown in Figure 1. DNA sequence analysis was generally carried out using Taq FS dye terminator cycle fluorescence-based sequencing on a Perkin-Elmer/Applied Biosystems Model 377A DNA Stretch Sequencer.

Construction of Mutant Receptors D4-NR and D4-Glg2 and Epitope-Tagged Receptors. The mutant D4-NR was constructed by restriction fragment replacement to delete amino acids 237 through 326 from the cytoplasmic loop i3 of the D4-4 receptor (Figure 1). In addition, D4-NR carries P327Q and T329A mutations in the reconstituted loop i3. The mutant D4-Glg2 was constructed using the "splicing by overlap extensions" PCR method (SOEing), which involves three successive rounds of PCR followed by directional cloning of the resulting restriction fragment (*9*). The D4-Glg2 gene encodes a chimeric receptor in which the cytoplasmic loop i3 of the D4 receptor (amino acid residues 218 through 341) is replaced by a portion of the cytoplasmic loop i3 of the rat glucagon receptor (amino acid residues 336 through 349) (Figure 6). Since satisfactory antibodies against the D4 dopamine receptor were not available, each of the synthetic genes (D4-2, D4-4, D4-7) and the mutant genes (D4-NR, D4-Glg2) was also prepared with a C-terminal epitope tag. A synthetic duplex encoding the 18 amino acid sequence (GKNPLGVRKTETSQVAPA) corresponding to the epitope of the 1D4 anti-rhodopsin monoclonal antibody was inserted after the codon for the C-terminal residue of each receptor construct. The epitope-tagged constructs were used only for immunoblot analysis of receptor expression.

Heterologous Expression of Synthetic Genes in Mammalian Cell Lines. The receptor genes were subcloned into the eukaryotic expression vector pMT3 (*10*) for expression in COS-1 cells and HEK 293T cells (*11, 12*), or pcDNA3 (InVitrogen) for expression in AtT-20 cells. Expression of dopamine receptor and mutant receptor genes in COS-1 and HEK 293T cells by transient transfection was performed as described using either Lipofectamine or Lipofectamine Plus (Gibco BRL) (*13*). Immunoblot analysis of expressed dopamine receptor and receptor mutants was carried out essentially as described (*14, 15*), except that the lysis buffer was 187.5 mM Tris-HCl, pH 6.8, 125 mM dithiothreitol, 6% (w/v) SDS, 30% (w/v) glycerol. The cell lysate was applied to a QIAshredder column (Qiagen) to shear genomic DNA followed by centrifugation at 15 000 rpm for 2 min at room temperature. The approximate levels of expression of the D4-2 receptor in the COS-1 cells and HEK 293T cells were 6.1 ± 2.8 pmol/mg of membrane protein and 1.2 ± 0.7 pmol/mg of membrane protein, respectively.

Preparation of Urea-Stripped COS Cell Membranes. Transiently transfected COS-1 cells from four 100-mm plates were washed once in phosphate-buffered saline (PBS) (137 mM NaCl, 8.0 mM Na_2HPO_4, 2.7 mM KCl, 1.5 mM KH_2-

PO_4) and collected in PBS supplemented with 100 μM 4-(2-aminoethyl)benzenesulfonyl fluoride hydrochloride (AEBSF) (Sigma). Plasma membranes were prepared as previously described (*14*). The final pellets were treated with a Dounce homogenizer, and the protein content of each sample was determined by the Bio-Rad Protein Assay (Bio-Rad). Aliquots with a protein content of 2 mg/mL were flash-frozen and stored at −80 °C. Chaotropic extraction of endogenous GTP-binding activity was carried out essentially as described (*16*). Briefly, plasma membranes from transfected COS-1 cells were incubated in 6 M urea in solution A (10 mM HEPES, pH 7.4, 1 mM EGTA) on ice for 30 min and sedimented at 70 000 rpm for 30 min at 4 °C. After a second extraction and centrifugation, the membrane pellet was washed once with solution A. The final pellet with a protein content of 0.4 mg/mL was treated with a Dounce homogenizer in buffer MS60+ (50 mM Tris-HCl, pH 7.5, 5 mM $MgCl_2$, 0.5 mM EDTA, 60 mM NaCl, 1 mM dithiothreitol, 10 μM GDP). Samples were flash-frozen in 40 μL aliquots and stored at −80 °C.

Binding of Spiperone to Transiently Transfected COS Cell Membranes. Transfected COS-1 cells from two 100-mm tissue culture plates were collected and resuspended in 0.5 mL of lysis buffer (5 mM Tris-HCl, pH 7.4, 2 mM EDTA). The cell suspension was passed 6 times through a 26 gauge needle and centrifuged at 15 000 rpm for 10 min at 4 °C. The pellet was resuspended in 0.5 mL of lysis buffer, treated with a Dounce homogenizer, and centrifuged as described above. The final pellet was resuspended using a Dounce homogenizer in 0.5 mL of binding buffer (50 mM Tris-HCl, pH 7.5, 0.5 mM EDTA, 5 mM $MgCl_2$, 5 mM KCl, 1.5 mM $CaCl_2$). Protein concentration was determined using the Bio-Rad Protein assay. Aliquots of the membrane preparation (5−40 μg of total protein) were added to duplicate assay tubes containing binding buffer supplemented with 2 mM L-ascorbic acid and increasing concentrations (10−1000 pM) of [^{3}H]-spiperone (15 Ci/mmol) (NEN). Nonspecific binding was determined by coincubation of a set of duplicate assay tubes of [^{3}H]-spiperone with 50 μM dopamine. Assay fractions were incubated in a final volume of 1 mL in the dark for 1 h at room temperature. The assays were terminated by filtration over Whatman GF/C filters presoaked in 0.05% polyethylenimine (Sigma) using a Brandel Cell Harvester. The filters were rinsed 3 times with 4 mL of ice-cold wash buffer (10 mM Tris-HCl, pH 7.4, 5 mM $MgCl_2$). Radioligand bound to the filters was detected by liquid scintillation counting using a Beckman LS 6500 counter. Nonlinear regression analysis was carried out to determine the K_D values given in Table 1.

Binding of Quinpirole to Transiently Transfected COS Cell Membranes. Membranes were prepared essentially as described above for spiperone binding with the exception that the final pellet was resuspended in 1.5 mL of quinpirole binding buffer (50 mM Tris-HCl, pH 7.5, 2 mM $MgCl_2$, 5 mM KCl, 2 mM $CaCl_2$). Protein concentration was determined using the Bio-Rad Protein assay. Aliquots of the membrane preparation (15−25 μg total protein) were added to duplicate assay tubes containing quinpirole binding buffer and increasing concentrations (0.1−25 nM) of [^{3}H]-quinpirole (37 Ci/mmol) (NEN). Nonspecific binding was determined by co-incubation of a set of duplicate assay tubes of [^{3}H]-quinpirole with 50 μM quinpirole. Assay fractions were incubated in a final volume of 1 mL for 5 h at room temperature. The assays were terminated by filtration over Whatman GF/B filters presoaked in 0.05% polyethylenimine (Sigma) using a Brandel Cell Harvester. The filters were rinsed 3 times with 4 mL of ice-cold wash buffer (10 mM Tris-HCl, pH 7.4). Radioligand bound to the filters was detected by liquid scintillation counting using a Beckman LS 6500 counter. The data were analyzed as Scatchard plots, and nonlinear regression analysis was carried out to determine K_D values as reported in Table 1.

Preparation and Characterization of Stable Cell Lines Expressing the Synthetic Dopamine Receptor Genes. AtT-20 cell lines derived from mouse pituitary tumors were stably transfected with D4 receptor genes cloned into pcDNA3 expression vectors using Lipofectamine. Selection was carried out using G418 (350 μg/mL).

Characterization of the Effect of Quinpirole on Bay K-Induced Calcium Flux in Stable Cell Lines Expressing the D4 Dopamine Receptor Variants. AtT-20 cells stably transfected with the D4-2, D4-4, D4-7, and D4-NR dopamine receptor variants were grown on 100-mm plates. The cells were harvested and loaded with the fluorophore Fluo-3-AM (Molecular Probes, Inc.) as described (*13*). Fluorescence due to binding of intracellular calcium to Fluo-3 was measured at room temperature in a Hitachi F-2000 fluorescence spectrophotometer using excitation and emission wavelengths of 505 and 525 nm, respectively. The L-type Ca^{2+} channel agonist (±)-Bay K 8644 (Calbiochem) was added to a final concentration of 1 μM. Inhibition of Bay K-induced Ca^{2+} flux was assayed by adding (−)-quinpirole hydrochloride (Research Biochemicals International, Inc.) or somatostatin to final concentrations of 50 or 10 μM, respectively.

Characterization of Quinpirole-Dependent Calcium Flux in Transiently Transfected HEK 293T Cells. Assays of intracellular calcium concentration in HEK 293T cells using Fluo-3 as an intracellular calcium-indicator dye were performed essentially as described (*13*). When used, Pertussis toxin (PTX) at 100 ng/mL was added to the transfected cells 18−24 h before harvesting. Studies were performed at least 3 times on independent samples to verify reproducibility. Changes in both the fluorescence peak heights and the actual $[Ca^{2+}]_i$ were used to generate dose−response curves. For graphical representation of an individual experiment, the data at each concentration of quinpirole were fit to a 4-parameter logistic function of the form: $f(x) = [(a - d)/(1 + (x/c)^b)] + d$ (Figure 5). The EC_{50} values were calculated from the inflection point (c) of the best-fit curve (Sigmaplot, Jandel Scientific Software) (Table 1). Quantification using either fluorescence peak heights or actual $[Ca^{2+}]_i$ gave essentially the same EC_{50} values. The peak heights at a given concentration were reproducible within a batch of cells assayed on a given day. Calcium flux in HEK 293T cells can be mediated through G_s-, G_i-, or G_q-dependent pathways (*13, 17*). Isoproterenol, somatostatin, and carbachol were used as specific control agonists to elicit G_s-, G_i-, and G_q-mediated calcium flux, respectively.

Purification of Retinal Transducin $\beta\gamma$ Subunits. Frozen bovine retinas were obtained from Lawson Co., Lincoln, NE. Holotransducin (G_t) was prepared essentially as described from crude bovine rod outer segments (*18*). However, the membranes were extracted with hypotonic buffer 2 additional times. G_t was released from the membranes by extraction

with hypotonic buffer supplemented with 100 μM GTP. G_t was purified using hexyl-agarose chromatography. The subunits were prepared essentially as described using Blue Sepharose CL-6B (Pharmacia) (*19*). Purified transducin $\beta\gamma$ subunits ($G_t\beta\gamma$) were dialyzed against 10 mM Hepes, pH 7.5, 2 mM $MgCl_2$, 1 mM DTT, 40% (v/v) glycerol and stored at −20 °C.

Preparation of Purified Recombinant G Protein Subunits. The following G protein subunits were expressed in *Sf*9 cells and purified essentially as described (*20*): $G_i\alpha1$, $G_i\alpha2$, $G_i\alpha3$, and $G_o\alpha$ (GenBank accession numbers M17527, M17528, M20713, and M17526, respectively).

Reconstitution of COS Cell Membranes with Purified G Proteins and Assay of Receptor-Stimulated GTPγS Binding. Frozen urea-stripped COS cell membranes (40 μL aliquots containing 0.4 mg/mL protein) were thawed on ice. CHAPS (3-[(3-cholamidopropyl)dimethylammonio]-1-propanesulfonate) (Anatrace, Inc.) was added to a final concentration of 0.03% (w/v). G protein subunits (1 μg per 16 μg of membrane protein) were added, and the mixture was incubated for 1 h at 0 °C. The mixture was brought to room temperature, and a 5 μL aliquot was transferred to an assay tube containing 20 μL of MS60 buffer (50 mM Tris-HCl, pH 7.5, 5 mM $MgCl_2$, 0.5 mM EDTA, 60 mM NaCl) including 0.5 nM [^{35}S]GTPγS (1250 Ci/mmol) (NEN), ±100 μM quinpirole. The assay mix was incubated for 16 min, and then terminated by rapid filtration over BA85 nitrocellulose filters (Schleicher & Schuell). The filters were rinsed 3 times with 4 mL of ice-cold wash buffer (10 mM Tris-HCl, pH 7.4, 5 mM $MgCl_2$, 60 mM NaCl). [^{35}S]GTPγS bound to the filters was measured by liquid scintillation counting. Binding in the absence of quinpirole was subtracted from binding in the presence of quinpirole to determine quinpirole-stimulated [^{35}S]GTPγS binding (Figures 7 and 8). Quinpirole-stimulated binding was observed only in the presence of added α and $\beta\gamma$ subunits (Figures 7 and 8). Reaction time-course experiments (not shown) determined that under these assay conditions, the amount of membrane preparation was limiting with respect to [^{35}S]GTPγS binding. Therefore, quinpirole-stimulated [^{35}S]GTPγS binding measures the degree of receptor-catalyzed [^{35}S]GTPγS binding by the added G protein α subunits, which do not saturate. The assay is sensitive to differences in G protein coupling among sets of receptors transfected in parallel and matched for receptor content, which is measured independently by immunoblot analysis and Scatchard analysis. The assay conditions are not designed to compare differences in specific activity among the G protein subtypes tested.

RESULTS

Design and Synthesis of Genes Encoding the Three Major Variants of the Human D4 Dopamine Receptor. Genes for three major variants of the human D4 dopamine receptor were designed and synthesized. The genes encode the D4-2, D4-4, and D4-7 dopamine receptors as indicated in Figure 1. These genes contain 2, 4, and 7 nonidentical hexadecapeptide units, respectively, in the center of the cytoplasmic loop linking TM helices 5 and 6. In addition, a gene encoding a deletion mutant that lacks the entire repeat region of loop i3 (D4-NR) was constructed to evaluate the potential role of the hexadecapeptide repeats in ligand binding and G protein coupling (Figure 1). The genes contain a large number of unique restriction sites to facilitate site-specific mutagenesis by a variety of approaches. The synthetic D4-2, D4-4, and D4-7 genes contained 25, 24, and 23 unique restriction sites, respectively. This compares with 11, 14, and 11 sites in the native D4-2, D4-4, and D4-7 nucleotide sequences, respectively. In addition, the G+C nucleotide content of the synthetic genes was reduced with the aim of enhancing levels of heterologous expression in mammalian cell lines. The synthetic D4-2, D4-4, and D4-7 genes had 48.2, 49.2, and 51.0% G+C content, respectively. This compares with 73.1, 74.1, and 75.3% G+C content in the native D4-2, D4-4, and D4-7 cDNAs, respectively.

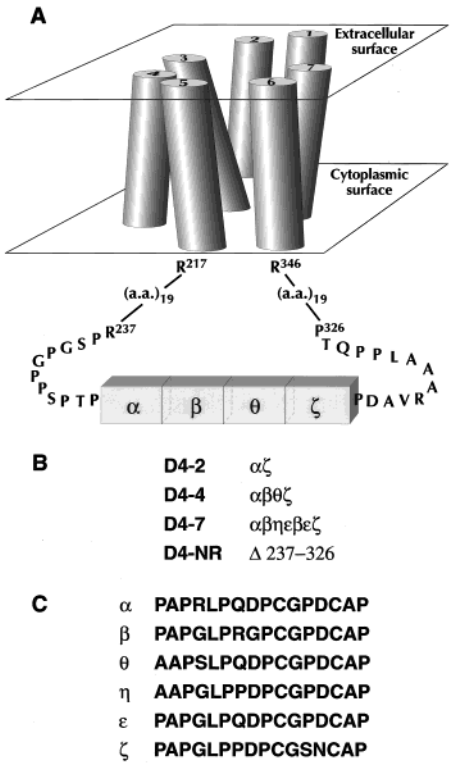

FIGURE 1: Schematic representation of the human D4 dopamine receptor variants and deletion mutant. (A) Seven putative TM helices are depicted as in previous models of GPCRs. The extracellular surface is toward the top, and the cytoplasmic surface is toward the bottom of the figure. For clarity, only the intracellular loop linking TM helices 5 and 6 is shown for the D4-4 receptor (Arg^{217} through Arg^{346}). The variable repeat region of the loop is depicted by boxes and comprises α, β, θ, and ζ repeats for the D4-4 receptor. (B) Compositions of the variable repeat regions of receptor variants D4-2, D4-4, and D4-7 are represented by Greek letters as shown. To construct the D4-NR receptor mutant, amino acid residues Arg^{237} through Pro^{326} were deleted. The D4-NR mutant lacks the variable repeat regions and the immediately flanking proline-rich sequences. (C) Hexadecapeptide sequences that make up the variable repeat regions in each of the D4 receptor variants are shown.

The genes were synthesized according to the basic strategy devised by Khorana and co-workers (*21*), which involves the total chemical synthesis of both upper and lower DNA strands. The only significant difference in the approach was that the synthetic DNA duplexes, which were joined in vitro by T4 DNA ligase-catalyzed joining reactions, were PCR-amplified to facilitate cloning. The longest gene (D4-7) was synthesized first in four fragments, which were sequenced and assembled. The other genes were completed by reconstructing the loop i3 region. The synthetic D4-2, D4-4, and

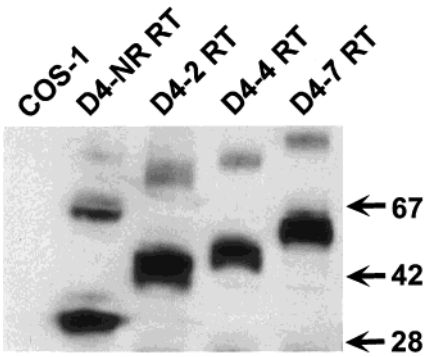

FIGURE 2: Immunoblot analysis of epitope-tagged D4 dopamine receptor synthetic genes expressed in transiently transfected COS-1 cells. COS-1 cells were transiently transfected with expression vectors containing the dopamine receptor variants or the D4-NR deletion mutant. Each receptor construct included an in-frame C-terminal epitope tag (RT) for the monoclonal antibody ID4. Cell lysates from one-tenth of a 100-mm plate were separated by 10% SDS−PAGE, transferred to membrane, and probed with the 1D4 antibody as described under Experimental Procedures. Immunoreactive bands were visualized by chemiluminescence. The numbered arrows indicate the apparent molecular masses (kDa) of molecular mass markers (not shown). There is no antibody cross-reactivity with untransfected COS-1 cells. The expressed receptors D4-NR RT, D4-2 RT, D4-4 RT, and D4-7 RT are visualized as bands migrating with apparent molecular masses of ~34.5, 41, 44, and 55 kDa, respectively. A band corresponding to receptor dimers can be appreciated for each construct.

D4-7 genes were 1161, 1257, and 1401 bp in length, respectively.

Expression of the Synthetic Genes in COS Cells. Each of the synthetic genes was expressed in COS-1 cells following transient transfection by a lipofection procedure. In addition, a version of each of the genes that contained a C-terminal epitope to the 1D4 monoclonal antibody was constructed and expressed. These epitope-tagged receptors could be probed by immunoblot analysis to evaluate expression as shown in Figure 2. The four receptors were expressed at relatively high levels in transiently transfected COS-1 cells. The expression levels are estimated to be about 6.1 ± 2.8 pmol/mg of membrane protein assuming that 100% of the cells are expressing the receptor. The main immunoreactive bands for D4-NR, D4-2, D4-4, and D4-7 migrated to positions corresponding to ~34.5, 41, 44, and 55 kDa, respectively. These values are consistent with the expected electrophoretic mobilities of the receptors. The bands are relatively broad, consistent with heterogeneous receptor glycosylation as expected. The bands collapse to single tighter bands upon treatment with N-glycosidase F, which cleaves all N-linked carbohydrate moieties (not shown). A potential receptor dimer band can be appreciated for each of the expressed receptors as is common for GPCRs (*15*).

Spiperone Binding to the Expressed Dopamine Receptors. Ligand saturation binding experiments were carried out under equilibrium conditions using the dopamine receptor antagonist [^{3}H]-spiperone and membranes from transiently transfected COS-1 cells. The data analysis indicated that all of the specific spiperone-binding sites for each receptor have the same affinity as expected. The K_D values determined from a series of individual binding experiments are presented in Table 1. The values for receptors D4-2, D4-4, and D4-7 (0.17 ± 0.06, 0.17 ± 0.01, and 0.14 ± 0.03 nM, respectively) are statistically identical and are consistent with previously reported values in COS-7 cells (*22*, *23*). This result indicates that the differences in the structure of loop i3 in the three receptor variants do not affect the antagonist ligand-binding pocket, which is located in the membrane-embedded domain of the receptor (*24*). The K_D value for spiperone binding by the deletion mutant D4-NR, 0.29 ± 0.06 nM, is slightly higher than that for the other native receptor variants.

Table 1: Pharmacological Parameters of Expressed D4 Dopamine Receptors[a]

receptor	K_D value[b] quinpirole binding (nM)	K_D value[b] spiperone binding (nM)	EC_{50} value,[c] calcium flux (nM)
D4-2	3.10 ± 1.70 (2)	0.17 ± 0.06 (5)	50.8 ± 26.2 (4)
D4-4	ND[d]	0.17 ± 0.01 (2)	200.0 ± 91.8 (3)
D4-7	ND[d]	0.14 ± 0.03 (2)	189.1 ± 97.7 (3)
D4-NR	ND[d]	0.29 ± 0.06 (5)	101.2 ± 33.3 (3)
D4-Glg2	1.45 ± 0.25 (2)	0.74 ± 0.19 (3)	NA[e]

[a] Values are given as mean ± SE. The number of independent experiments is given in parentheses. [b] The K_D values were determined as described under Experimental Procedures. [c] The effective quinpirole concentrations at 50% stimulation of calcium flux (EC_{50} values) were determined as shown in Figure 5. The average EC_{50} values are not statistically different at $p < 0.05$ (Student's *t*-test). [d] ND, not determined. [e] The cells expressing the D4-Glg2 chimeric receptor did not flux calcium in response to quinpirole.

Quinpirole-Induced Inhibition of Bay K-Mediated Calcium Flux in Stable Cell Lines Expressing the Dopamine Receptor Variants. A hallmark of signal transduction by the D4 dopamine receptor is its ability to inhibit Bay K-mediated calcium flux in cells containing plasma membrane L-type calcium channels. To test for this activity, stable cell lines expressing the synthetic genes were prepared in AtT-20 cells. The cells displayed cell-surface expression of the receptors as judged by spiperone-binding experiments (not shown). The results of a representative experiment are shown in Figure 3 for the stably expressed D4-7 receptor variant. Bay K treatment resulted in an increase in intracellular calcium concentration as assayed by a time-dependent increase in Fluo-3 fluorescence measured at 525 nm. The fluorescence reached a plateau, then returned to base line upon injection of the dopamine-receptor agonist quinpirole. Quinpirole treatment alone had no effect on $[Ca^{2+}]_i$ as judged by Fluo-3 fluorescence. Identical quinpirole-induced inhibition of Bay K-mediated calcium flux was seen for the cell lines expressing the D4-2, D4-4, and D4-NR receptor variants (data not shown).

Quinpirole-Induced Calcium Flux in HEK 293T Cells Expressing the Dopamine Receptor Variants. We next evaluated the pharmacology and G protein coupling characteristics of D4 dopamine receptors expressed in the HEK 293T cells by measuring receptor-mediated increases in $[Ca^{2+}]_i$. Transiently transfected cells were loaded with the calcium-sensitive dye Fluo-3. Heterologous expression of the synthetic D4-4 dopamine receptor resulted in an increase in Fluo-3 fluorescence upon treatment of the cells with the dopamine receptor agonist quinpirole (Figure 4, upper panel). Nontransfected HEK 293T cells did not show a response to quinpirole (not shown). The quinpirole-induced fluorescence was characterized by a rapid increase, followed by an apparent exponential decay to a new base line slightly above the original prestimulation levels. The resetting of the base

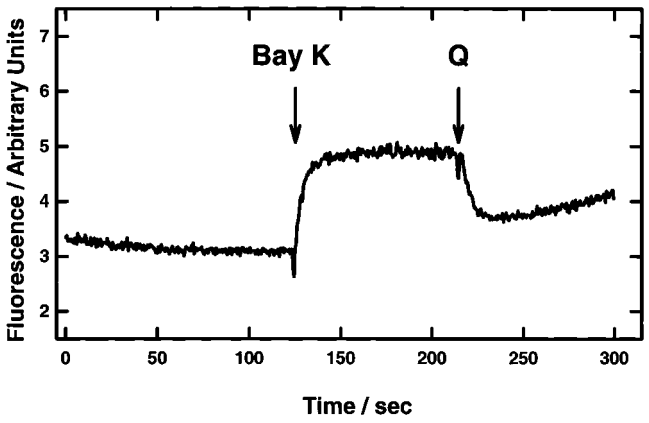

FIGURE 3: Quinpirole-induced inhibition of Bay K 8644-mediated Ca^{2+} flux. AtT-20 cells were stably transfected with the synthetic gene for the human D4-7 dopamine receptor. The stable cell line was loaded with Fluo-3 and assayed as described under Experimental Procedures. The trace represents the level of Fluo-3 fluorescence emitted over time by the cells suspended in solution. The L-type Ca^{2+} channel agonist (±)-Bay K 8644 was added to a final concentration of 1 μM as indicated. The dopamine receptor agonist (−)-quinpirole hydrochloride was added to a final concentration of 50 μM as indicated. Quinpirole treatment caused inhibition of the Bay K-induced Ca^{2+} flux. Similar results were obtained in cell lines expressing the synthetic genes for the D4-2, D4-4, and D4-NR receptor variants.

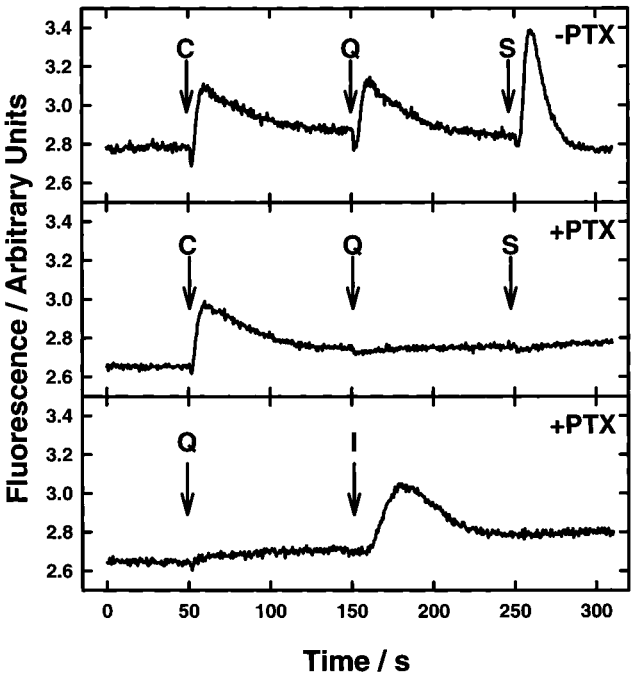

FIGURE 4: Pertussis toxin sensitivity of the quinpirole-dependent elevation of intracellular calcium concentration in transiently transfected HEK 293T cells. HEK 293T cells were transiently transfected with the synthetic gene for the human D4-4 dopamine receptor. Cells were loaded with the calcium-binding fluorophore Fluo-3 as described under Experimental Procedures. The traces represent the level of fluorescence in arbitrary units emitted over time by the transfected cells suspended in solution. In the upper trace (−PTX), cells were pretreated with water. In the middle trace (+PTX), cells were pretreated with 100 ng/mL PTX. The arrows labeled with letters C, Q, and S signify the addition of carbachol (1 mM), quinpirole (0.1 mM), and somatostatin (1 mM, final concentration), respectively. In the lower trace (+PTX), cells were pretreated with 100 ng/mL PTX, and the arrows labeled with letters Q and I signify the addition of quinpirole (1.0 mM) and isoproterenol (10 nM, final concentration), respectively. Treatment with PTX abolished the calcium flux mediated by quinpirole or somatostatin but had no effect on the carbachol- or isoproterenol-induced calcium signaling. Identical results were obtained in cells expressing the genes for the D4-2 and D4-7 dopamine receptors.

line is most likely caused by capacitative calcium entry (CCE) due to influx of extracellular calcium after depletion of hormone-sensitive intracellular stores (*25*, *26*). The quinpirole-induced response resembled the carbachol-induced response in both its magnitude and the presence of CCE, which was not seen in the somatostatin-induced fluorescence peak. Treatment with PTX prevented the agonist-dependent increase in $[Ca^{2+}]_i$ by somatostatin and quinpirole, but not by carbachol or isoprotenenol, indicating that the expressed D4-4 dopamine receptors coupled to endogenous $G_i\alpha$ or $G_o\alpha$ in the HEK 293T cells (Figure 4, lower panels). Identical results were obtained for the other dopamine receptor variants (D4-2, D4-4, and D4-7) and for D4-NR.

As the concentration of quinpirole was decreased, a dose-dependent decrease in fluorescence peak height was observed, with an associated increase in both the time-to-peak and the half-life of the exponential decay of the $[Ca^{2+}]_i$ signal. Accurate dose−response data were collected by measuring the effects of various concentrations of quinpirole on the $[Ca^{2+}]_i$ fluorescence signal. Dose−response curves are shown in Figure 5 for the three D4 receptor variants and the deletion mutant D4-NR. EC_{50} values determined from sets of dose−response curves are presented in Table 1. The average EC_{50} values for the quinpirole-induced calcium flux range from 50.8 nM for D4-2 to 200.0 nM for D4-4. However, when considering the standard error (Table 1), the differences among the EC_{50} values for the four receptors are not statistically significant at the 0.05 confidence limit.

Preparation and Expression of a Chimeric D4 Dopamine Receptor Containing a Cytoplasmic Loop i3 Replacement. Since there were no significant differences among the D4 dopamine receptor variants or D4-NR in G protein-mediated calcium flux, a mutant was constructed to confirm the hypothesized role of loop i3 in dopamine receptor coupling to G proteins. In the chimeric receptor D4-Glg2, amino acid residues 218−341 of the D4-4 dopamine receptor were replaced by amino acid residues 336−349 from loop i3 of the rat glucagon receptor (Figure 6A). Loop i3 is known to mediate G_s coupling to the glucagon receptor (*13*). Compared with the D4-NR mutant (Δ237−326), the D4-Glg2 mutant had additional residues replaced at both the N-terminal and C-terminal ends of loop i3. The D4-Glg2 gene was expressed in COS-1 cells. Expression was confirmed by immunoblot analysis using an epitope-tagged version of the receptor (not shown). The level of expression of the D4-Glg2 receptor was comparable to that of the receptor variants as judged by immunoblot analysis. The D4-Glg2 receptor was found on the surface of the HEK 293T cells as judged by ligand-saturation binding experiments (see below) and immunofluorescence microscopy (not shown). The COS cell membranes containing the expressed D4-Glg2 receptor bound spiperone in equilibrium ligand-saturation binding assays with a K_D value of 0.74 ± 0.19 nM, which was just slightly higher than values obtained for the other dopamine receptors studied (Table 1). The membranes containing the expressed D4-Glg2 receptor also bound quinpirole in equilibrium ligand-saturation binding assays with a K_D value of 1.45 ± 0.25 nM, which was indistinguishable from the K_D value

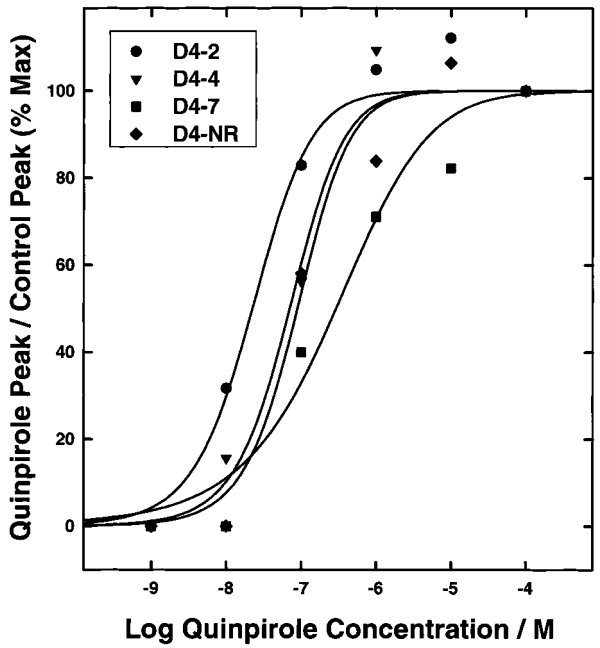

FIGURE 5: Dose−response curves for the quinpirole-mediated calcium flux in HEK 293T cells transiently transfected with synthetic genes for the human D4 dopamine receptor variants (D4-2, D4-4, D4-7) or deletion mutant (D4-NR). Calcium flux was measured at various concentrations of quinpirole. The data for each receptor were normalized with 100% activity defined as the activity at the highest concentration of quinpirole measured (100 μM). Each trace is representative of at least three independent sets of experiments. The effective concentrations at 50% maximal stimulation of calcium flux (EC_{50} values) were determined as described under Experimental Procedures and are reported in Table 1.

obtained with the D4-2 receptor (Table 1). When transiently expressed in HEK 293T cells, the D4-Glg2 receptor failed to induce calcium flux in response to quinpirole even at high concentrations (Figure 6B).

Reconstitution of Expressed Dopamine Receptor Variants with Recombinant G Protein α *Subunits*. Urea-stripped COS cell membranes containing expressed dopamine receptor variants were reconstituted with recombinant $G_i\alpha$ subunits purified from baculovirus-infected *Sf*9 insect cells. Quinpirole-stimulated GTPγS binding was assayed to test for differences in coupling of specific G protein subtypes ($G_i\alpha1$, $G_i\alpha2$, $G_i\alpha3$) to specific receptor variants (D4-2, D4-4, D4-7). The results are presented in Figure 7. A mixture of membranes containing the three receptor variants was used to perform control experiments on isolated subunits. When added to the D4-mix control membranes, purified transducin $\beta\gamma$ subunits ($G_t\beta\gamma$) alone, purified $G_i\alpha1$ subunits alone, purified $G_i\alpha2$ subunits alone (not shown), and purified $G_i\alpha3$ subunits alone (not shown) did not show a quinpirole-induced increase in GTPγS binding. However, the combination of $G_t\beta\gamma$ and $G_i\alpha1$ with membranes containing individual receptor variants caused a quinpirole-induced increase in GTPγS binding. There was no difference in quinpirole-induced coupling of $G_i\alpha1$ to membranes containing D4-2, D4-4, or D4-7 receptors. Likewise, there was no difference in quinpirole-induced coupling of $G_i\alpha2$ or $G_i\alpha3$ to membranes containing D4-2, D4-4, or D4-7 receptors. The data in Figure 7 are compiled from three to seven reconstitution experiments on the same recombinant G protein preparations.

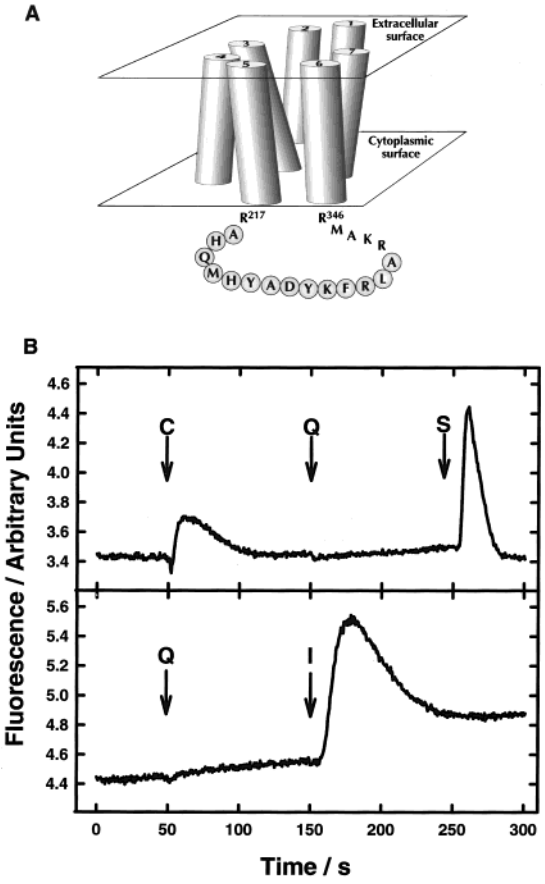

FIGURE 6: Replacement of the cytoplasmic loop i3 of the D4 dopamine receptor prevents G protein coupling. (A) A chimeric receptor (D4-Glg2) was constructed in which the cytoplasmic loop i3 of the D4-4 dopamine receptor was replaced with the corresponding loop of the glucagon receptor. Seven putative TM helices are shown to represent the D4-Glg2 chimera with the extracellular surface toward the top and the cytoplasmic surface toward the bottom of the figure. Amino acids 218−341 of the D4-4 dopamine receptor were replaced by loop i3 of the rat glucagon receptor (amino acid residues 336−349). The sequence from the glucagon receptor is shown in circles. For clarity, only the intracellular loop linking TM helices 5 and 6 is shown. (B) HEK 293T cells were transiently transfected with the gene for the D4-Glg2 receptor and then loaded with Fluo-3. The traces represent the level of fluorescence in arbitrary units emitted over time by the transfected cells suspended in solution. In the upper trace, the arrows labeled with letters C, Q, and S signify the addition of carbachol (1 mM), quinpirole (0.1 mM), and somatostatin (1 mM, final concentration), respectively. In the lower trace, the arrows labeled with letters Q and I signify the addition of quinpirole (1.0 mM) and isoproterenol (10 nM, final concentration), respectively. The behavior of the D4-4 dopamine receptor under identical conditions is shown in Figure 4. The D4-Glg2 receptor was expressed on the cell surface and bound spiperone and quinpirole (Table 1). However, it failed to couple to cellular G proteins to cause calcium signaling.

In all cases, the coupling of $G_i\alpha$ to receptor was dependent on $G\beta\gamma$ as expected. The experiments were designed to evaluate potential differences in the coupling of each $G_i\alpha$ subtype to the three receptor variants. The results show that each $G_i\alpha$ subtype couples equally well to the three receptor variants. The D4-2, D4-4, and D4-7 receptors also coupled to recombinant purified $G_o\alpha$ in the presence of $G\beta\gamma$ (data not shown).

$G_i\alpha$ coupling to the two mutant dopamine receptors D4-NR and D4-Glg2 was also measured in the reconstitution assay (Figure 8). Quinpirole-induced GTPγS binding in the

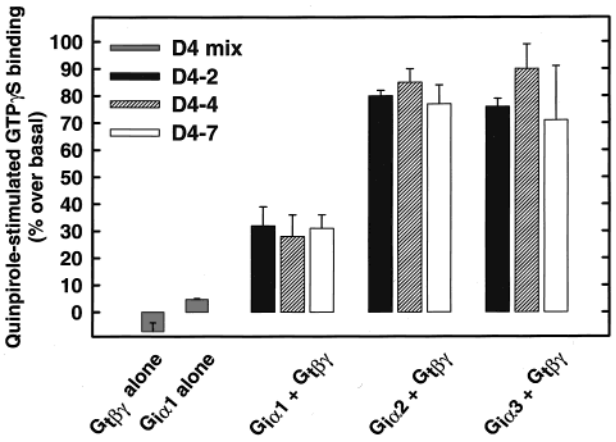

FIGURE 7: Quinpirole-stimulated GTPγS binding to membranes containing expressed G protein subunits and dopamine receptor variants. COS-1 cells were transiently transfected with synthetic human dopamine receptor genes (D4-2, D4-4, D4-7). Cellular membranes were isolated and urea-stripped. The urea-stripped membranes were reconstituted with various combinations of transducin $\beta\gamma$ subunits purified from bovine rod outer segments ($G_t\beta\gamma$) and recombinant $G_i\alpha$ subunits purified from *Sf*9 cells ($G_i\alpha1$, $G_i\alpha2$, $G_i\alpha3$). Quinpirole-stimulated [^{35}S]GTPγS binding was measured as described under Experimental Procedures. The bars represent mean percent of quinpirole-stimulated GTPγS binding over basal levels ± SE ($n = 3-7$ experiments). GTPγS binding occurred only when both G protein α and $\beta\gamma$ subunits were present. There was no significant difference in coupling among the receptor variants for any particular G_i subtype as judged by the Student's paired *t*-test.

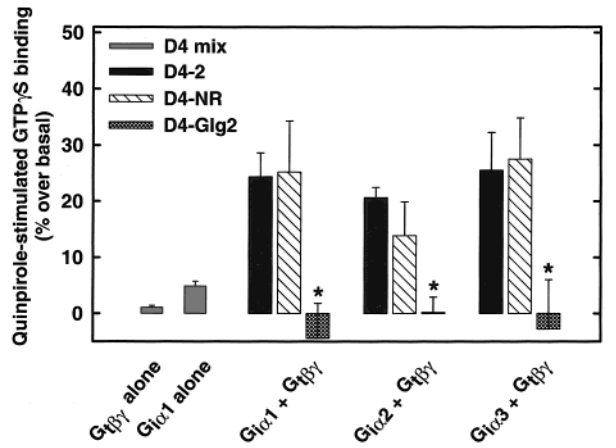

FIGURE 8: Quinpirole-stimulated GTPγS binding to membranes containing expressed G protein subunits and dopamine receptor mutants. COS-1 cells were transiently transfected with synthetic human dopamine receptor mutants (D4-NR, D4-Glg2). The D4-2 receptor gene was expressed as a control. Cellular membranes were isolated and urea-stripped. The urea-stripped membranes were reconstituted with various combinations of transducin $\beta\gamma$ subunits purified from bovine rod outer segments ($G_t\beta\gamma$) and recombinant $G_i\alpha$ subunits purified from *Sf*9 cells ($G_i\alpha1$, $G_i\alpha2$, $G_i\alpha3$). Quinpirole-stimulated [^{35}S]GTPγS binding was measured as described under Experimental Procedures. The bars represent mean percent of quinpirole-stimulated GTPγS binding over basal levels ± SE ($n = 3-7$ experiments). GTPγS binding occurred only when both G protein α and $\beta\gamma$ subunits were present. There was no significant difference in coupling to any of the G_i subtypes between the D4-2 receptor and the D4-NR loop i3 deletion mutant. The D4-Glg2 mutant failed to stimulate GTPγS binding by the $G_i\alpha$ subunits. * indicates a difference from D4-2 and D4-NR at $P < 0.05$ (Student's paired *t*-test).

presence of membranes containing each of the mutant receptors was compared to that in the presence of membranes containing the D4-2 receptor. The D4-NR receptor coupled to each of the $G_i\alpha$ subtypes. The coupling efficiency was equal to that of the D4-2 receptor. The deletion mutant D4-Glg2 failed to induce GTPγS binding in the presence of quinpirole. These results are consistent with the results of the calcium flux assays in HEK 293T cells (Figure 6).

DISCUSSION

We designed and synthesized genes for three major human D4 receptor variants: D4-2, D4-4, and D4-7. The genes are identical except in the region encoding the middle of the cytoplasmic loop linking TM helices 5 and 6, which contains a variable number of related, but not identical hexadecapeptide repeat elements. The synthesis and expression of a D4-4 receptor gene designed primarily to reduce G+C content by 14% was reported previously (*27*). The D4 genes constructed for the present study had considerably less G+C content with an average aggregate reduction of 24.7% for the three genes. The synthesis of a gene for the D4-2 receptor was also reported (*28*). It was expressed in CHO and HEK 293 cells and mediated inhibition of forskolin-stimulated cAMP accumulation.

The synthetic genes for D4-2, D4-4, D4-7, and D4-NR, a mutant receptor lacking all of the repeat elements in loop i3, were transiently expressed in COS-1 cells (Figure 1). Saturation ligand-binding experiments were carried out on the four expressed D4 receptors using the D2-like receptor antagonist spiperone. Nonlinear regression analysis yielded K_D values of 0.14−0.17 nM for the D4-2, D4-4, and D4-7 receptors. The K_D value for the D4-NR receptor was slightly higher at 0.29 nM. These values are similar to those previously reported. Receptor variants expressed in CHO cells gave K_D values for spiperone binding of 97 pM (*29*) and 310 pM (*30*). Asghari et al. (*29*) also evaluated a loop i3 deletion mutant that would correspond to Δ253−315 in the numbering in Figure 1. They reported no significant differences in the pharmacology of ligand binding for this mutant receptor.

To evaluate signal transduction by the expressed D4 receptors, we first prepared stable cell lines expressing each of the synthetic genes including D4-NR. AtT-20 cells derived from mouse pituitary tumor were chosen so that dopamine receptor signaling could be readily assessed in whole cells. These cells contain L-type calcium channels that respond to Bay K by increasing calcium conductance. Quinpirole-induced inhibition of Bay K-mediated calcium flux is a useful assay of D4 receptor signaling. Bay K treatment resulted in an increase in calcium-induced fluorescence, and subsequent treatment with quinpirole inhibited the Bay K effect as shown in Figure 3. Each of the stable cells lines showed identical quinpirole-induced inhibition of Bay K-mediated calcium flux. These results suggest that cellular signaling in the AtT-20-derived cell lines is the same for each of the receptor variants.

Dopamine D4 receptors most likely couple to the $G_i\alpha$ class of G proteins (*5*). Classically, D4 receptor activation inhibits forskolin-stimulated cAMP accumulation. D4 receptor activation may also inhibit Bay K-induced calcium flux by L-type dihydropyridine-sensitive calcium channels to lower $[Ca^{2+}]_i$, but only in cells expressing such channels. Rather than focusing on assays measuring the inhibitory effects of D4 receptor signaling on amplified second messenger

systems, we developed a cell-based assay system with a positive readout to study the pharmacology and signaling of D4 receptors. HEK 293T cells show a transient increase in $[Ca^{2+}]_i$ upon GPCR-mediated stimulation of either $G_s\alpha$, $G_i\alpha$, or $G_q\alpha$ (*13*). The $[Ca^{2+}]_i$ flux can be readily assayed by monitoring the steady-state fluorescence of Fluo-3 as a function of time in a population of cells suspended in a physiological buffer. HEK 293T cells are nonexcitable and do not express L-type, dihydropyridine-sensitive plasma membrane Ca^{2+} channels (*31*). Therefore, the biochemical pathways leading from $G_s\alpha$, $G_i\alpha$, and $G_q\alpha$ to changes in $[Ca^{2+}]_i$ are not the same as those described in so-called excitable cell types or tissues (*32*). $[Ca^{2+}]_i$ flux in the HEK 293T cells is most likely mediated by IP_3 receptors in the ER membrane.

We used somatostatin as a positive control for G_i-mediated $[Ca^{2+}]_i$ flux in the HEK 293T cells (Figure 4). The five somatostatin receptor subtypes have been shown to couple only to $G_i\alpha$ (*33*). $G_i\alpha$-mediated decreases in $[Ca^{2+}]_i$ were observed in cells containing dihydropyridine-sensitive, voltage-gated Ca^{2+} channels (*34*). However, in COS-7 cells, somatostatin receptors were shown to increase $[Ca^{2+}]_i$ via $G\beta\gamma$ activation of PLCβ (*35*), and similar effects have been reported in other cell types (*36*−*39*). $[Ca^{2+}]_i$ increases were also caused by the $G_i\alpha$-coupled D2 dopamine receptor through $G\beta\gamma$-mediated stimulation of PLCβ in mouse fibroblast Ltk- cells (*40*). In summary, in HEK 293T cells, the increase in $[Ca^{2+}]_i$ from intracellular stores mediated by somatostatin most likely results from $G_i\beta\gamma$ activation of PLCβ. The essential element of the assay used here is that increases in $[Ca^{2+}]_i$ mediated by more than one G protein subtype can be measured in the same cell preparation. Furthermore, the results can be quantified to produce dose−response curves for agonist ligands that use the same readout (i.e., increase in $[Ca^{2+}]_i$).

Preincubation of HEK 293T cells with PTX causes ADP-ribosylation of $G_i\alpha$ when it is complexed with its $\beta\gamma$ heterodimer. This modification prevents receptor-catalyzed nucleotide exchange. Thus, PTX can be used selectively to inhibit receptor coupling to $G_i\alpha$. Although all G_i family members are PTX-sensitive, not every $G_i\alpha$ subtype couples to any given G_i-linked receptor. For example, PTX-insensitive mutants of $G_i\alpha$ subunits were used to show that endogenous somatostatin receptors in GH_4C_1 cells inhibited adenylyl cyclase by coupling to $G_i\alpha1$ and $G_i\alpha3$, but not to $G_i\alpha2$. However, in the same cell type, $D2_s$ dopamine receptors signaled through $G_i\alpha2$ and not the other $G_i\alpha$ isoforms (*41*). Thus, not only do individual receptors demonstrate specificity for a given G protein α subtype, but not all $G_i\alpha$-coupled receptors activate the same set of $G_i\alpha$ isoforms, even in the same cell.

PTX selectively eliminated calcium signaling by quinpirole in cells transfected with each of the D4 receptors, indicating that the heterologously expressed receptors coupled exclusively to members of the $G_{i/o}\alpha$ class to mediate $[Ca^{2+}]_i$ flux (Figure 4). Untransfected HEK 293T cells showed no calcium flux in response to quinpirole. The fluorescence assay was also used to quantify pharmacological parameters related to the expressed D4 receptors. We determined dose−response curves for changes in $[Ca^{2+}]_i$ as a function of quinpirole concentration (Figure 5). The EC_{50} values derived from these curves ranged from 50.8 to 200.0 nM (Table 1). When the standard errors are considered, the values for D4-4, D4-7, and D4-NR are statistically identical. Only the D4-2 receptor shows a slightly lower EC_{50} value compared with those of D4-4 and D4-7.

Since the D4-NR receptor appeared to signal normally with an EC_{50} value of 101.2 nM (Figure 5 and Table 1), a chimeric receptor was constructed in which the entire loop i3 of the D4 receptor (residues 218−341) was replaced by the corresponding loop of the glucagon receptor (Figure 6A). This receptor (D4-Glg2) was expressed on the cell surface and bound spiperone and quinpirole (Table 1). D4-Glg2 failed to mediate quinpirole-dependent $[Ca^{2+}]_i$ flux (Figure 6B), showing that the membrane-proximal segments of loop i3 are required for proper G protein coupling. The replacement of the D4 receptor loop i3 by that of the glucagon receptor did not confer the ability of D4-Glg2 to couple to G_s as judged by the absence of quinpirole-dependent $[Ca^{2+}]_i$ flux (Figure 6B). Since the D4-NR receptor (Δ237−326) functioned normally, the regions of loop i3 flanking the hexadecapeptide repeats are specifically required for G_i protein coupling. Namely, residues 218−237 and 326−341 must facilitate receptor coupling to G_i. Oldenhof et al. (*3*) also characterized several loop i3 deletion mutants. In particular, they found that agonist stimulation of a deletion mutant D4(Δ221−337) did not block forskolin-stimulated increases in cAMP in CHO-K1 cells.

The calcium flux assay appears to be superior to existing assays that measure quinpirole-induced inhibition of forskolin-mediated cAMP accumulation to obtain EC_{50} values for agonist-induced dopamine receptor activity. These results demonstrate that synthetic dopamine receptor genes transiently expressed in HEK 293T cells can use endogenous signaling machinery to cause an agonist-dependent increase in $[Ca^{2+}]_i$. The coupling of the D4 receptor to calcium signaling is through a PTX-sensitive G protein. The exact mechanism of quinpirole-induced $[Ca^{2+}]_i$ flux is not fully established and is the subject of ongoing study.

Expressed dopamine receptor variants were reconstituted with recombinant G protein α subunits. Membranes that contained each of the D4 variants or a mixture of the three variants were tested initially (Figure 7). The membranes showed no quinpirole-induced binding of GTPγS when reconstituted with any of three purified recombinant $G_i\alpha$ subtypes ($G_i\alpha1$, $G_i\alpha2$, or $G_i\alpha3$) alone, or with the purified $G_i\beta\gamma$ heterodimer alone. Both $G_i\alpha$ and $G_i\beta\gamma$ subunits were required for receptor-catalyzed guanine nucleotide exchange. $G_i\beta\gamma$ is known to support the coupling of $G_i\alpha$ subunits to GPCRs (*42*). Each of the $G_i\alpha$ subtypes tested ($G_i\alpha1$, $G_i\alpha2$, or $G_i\alpha3$) coupled to quinpirole-stimulated D4-2, D4-4, and D4-7 receptors. There was no evidence of a quantitative difference in coupling of a particular $G_i\alpha$ subtype to a particular D4 receptor variant (Figure 7). For example, $G_i\alpha1$ coupled equally well to D4-2, D4-4, and D4-7. A direct quantitative comparison of the specific activities of the individual recombinant $G_i\alpha$ subunits is difficult due to variations among different preparations. However, our experience suggests that there is no significant preference among the D4 receptors for any one of the $G_i\alpha$ subtypes. A previous reconstitution study of the D2 dopamine receptor suggested selective coupling to $G_i\alpha2$ (*43*).

The evaluation of the D4-NR and D4-Glg2 mutants is presented in Figure 8. Mutant receptor D4-NR coupled

normally to $G_i\alpha1$, $G_i\alpha2$, and $G_i\alpha3$. However, mutant receptor D4-Glg2 failed to couple to each of the $G_i\alpha$ subunits tested in the reconstitution assay. These results are consistent with the results from the cell-based calcium flux assay (Figure 6). The results of the direct biochemical reconstitution assay confirm the role of loop i3 in D4 receptor coupling to G_i. Furthermore, we show direct evidence that $G_i\alpha2$ can couple to each of the four D4 receptor variants tested. This latter result appears to be at odds with earlier work reporting that the rat D4 receptor did not appear to couple to $G_i\alpha2$ in MN9D cells (*44*, *45*). O'Hara et al. (*45*) reported that the rat D4 dopamine receptor did not couple to $G_i\alpha2$ or $G_o\alpha A$ in MN9D cells using an assay of adenylyl cyclase inhibition. It should be noted that we did not study the rat D4 receptor specifically. Tang et al. (*44*) studied D4 dopamine receptor stimulation in CCL1.3 cells (a mouse Ltk- fibroblast line) and MN9D cells (a mouse neuronal mesencephalic line). They found no effect of dopamine on inositol phosphate metabolism in either cell line. However, they found PTX-sensitive inhibition of adenylyl cyclase in the MN9D cells. Both cell lines displayed high levels of $G_i\alpha2$, but no $G_i\alpha1$, $G_i\alpha3$, or $G_o\alpha$. Since it was considered unlikely that the receptors would couple to $G_i\alpha2$ in one cell type and not another, they concluded that the D4 receptor coupled to a novel PTX-sensitive G protein in the MN9D cells and not to $G_i\alpha2$. Subsequently, Yamaguchi et al. (*46*) reported the presence of cone transducin $G_t\alpha2$ in MN9D cells. They showed that D4 coupled to a mutant of cone $G_t\alpha$ that was resistant to PTX to inhibit forskolin-stimulated adenylyl cyclase activity with quinpirole. We found that the D4 receptor variants do couple to purified bovine rod transducin (not shown), and we expect that they would also couple to human cone transducin, whose α subunit is highly homologous.

In conclusion, we find no significant effect of the D4 receptor loop i3 polymorphism on antagonist or agonist binding. In a cell-based assay in HEK 293T cells, the D4 receptors couple exclusively to a PTX-sensitive pathway to mediate calcium flux. The regions of loop i3 near membrane borders of both TM helices 5 and 6 are required for G protein coupling as demonstrated both in cell-based calcium flux assays and in reconstitution assays. Our results show that each D4 receptor variant is capable of coupling to several $G_i\alpha$ subtypes. Furthermore, there is no evidence of any quantitative difference in G protein coupling related to the number of hexadecapeptide repeats in loop i3. In future work, we intend to reconstitute the D4 receptor with other $G\alpha$ classes, such as $G_t\alpha2$, and to identify the precise mechanism of D4-mediated calcium flux. In addition, the role of loop i3 as a potential ligand for SH3-binding domains and other cellular signaling molecules will be investigated.

ACKNOWLEDGMENT

We thank Cliff Sonnenbrot for oligonucleotide synthesis and Dr. Patrick Allen for the gift of HEK 293T cells. We also thank Dr. Chris Min, Dr. Tanya Zvyaga, and Ethan Marin for suggestions and advice.

REFERENCES

1. Fraser, C. M., Lee, N. H., Pellegrino, S. M., and Kerlavage, A. R. (1994) *Prog. Nucleic Acid Res. Mol. Biol. 49*, 113−156.
2. Gilman, A. G. (1987) *Annu. Rev. Biochem. 56*, 615−649.
3. Oldenhof, J., Vickery, R., Anafi, M., Oak, J., Ray, A., Schoots, O., Pawson, T., von Zastrow, M., and Van Tol, H. H. (1998) *Biochemistry 37*, 15726−15736.
4. Yu, H., Chen, J. K., Feng, S., Dalgarno, D. C., Brauer, A. W., and Schreiber, S. L. (1994) *Cell 76*, 933−945.
5. Van Tol, H. H., Bunzow, J. R., Guan, H. C., Sunahara, R. K., Seeman, P., Niznik, H. B., and Civelli, O. (1991) *Nature 350*, 610−614.
6. Ferretti, L., Karnik, S. S., Khorana, H. G., Nassal, M., and Oprian, D. D. (1986) *Proc. Natl. Acad. Sci. U.S.A. 83*, 599−603.
7. Sakmar, T. P., and Khorana, H. G. (1988) *Nucleic Acids Res. 16*, 6361−6372.
8. Carruthers, C. J. L., and Sakmar, T. P. (1995) *Methods Neurosci. 25*, 322−344.
9. Vallejo, A. N., Pogulis, R. J., and Pease, L. R. (1995) *PCR Primer: A Laboratory Manual*, Cold Spring Harbor Laboratory Press, Cold Spring Harbor, NY.
10. Franke, R. R., Sakmar, T. P., Oprian, D. D., and Khorana, H. G. (1988) *J. Biol. Chem. 263*, 2119−2122.
11. DuBridge, R. B., Tang, P., Hsia, H. C., Leong, P. M., Miller, J. H., and Calos, M. P. (1987) *Mol. Cell. Biol. 7*, 379−387.
12. Pear, W. S., Nolan, G. P., Scott, M. L., and Baltimore, D. (1993) *Proc. Natl. Acad. Sci. U.S.A. 90*, 8392−8396.
13. Cypess, A. M., Unson, C. G., Wu, C. R., and Sakmar, T. P. (1999) *J. Biol. Chem. 274*, 19455−19464.
14. Unson, C. G., Cypess, A. M., Kim, H. N., Goldsmith, P. K., Carruthers, C. J., Merrifield, R. B., and Sakmar, T. P. (1995) *J. Biol. Chem. 270*, 27720−27727.
15. Carruthers, C. J., Unson, C. G., Kim, H. N., and Sakmar, T. P. (1994) *J. Biol. Chem. 269*, 29321−29328.
16. Hellmich, M. R., Battey, J. F., and Northup, J. K. (1997) *Proc. Natl. Acad. Sci. U.S.A. 94*, 751−756.
17. Wayman, G. A., Hinds, T. R., and Storm, D. R. (1995) *J. Biol. Chem. 270*, 24108−24115.
18. Fung, B. K. K., and Nash, C. R. (1983) *J. Biol. Chem. 258*, 10503−10510.
19. Shichi, H., Yamamoto, K., and Somers, R. L. (1984) *Vision Res. 24*, 1523−1531.
20. Graber, S. G., Figler, R. A., and Garrison, J. C. (1992) *J. Biol. Chem. 267*, 1271−1278.
21. Khorana, H. G. (1979) *Science 203*, 614−625.
22. Van Tol, H. H. M., Wu, C. M., Guan, H.-C., Ohara, K., Bunzow, J. R., Civelli, O., Kennedy, J., Seeman, P., Niznik, H. G., and Jovanovic, V. (1992) *Nature 358*, 149−152.
23. Asghari, V., Schoots, O., van Kats, S., Ohara, K., Jovanovic, V., Guan, H. C., Bunzow, J. R., Petronis, A., and Van Tol, H. H. (1994) *Mol. Pharmacol. 46*, 364−373.
24. Ji, T. H., Grossmann, M., and Ji, I. (1998) *J. Biol. Chem. 273*, 17299−17302.
25. Putney, J. W., Jr. (1986) *Cell Calcium 7*, 1−12.
26. Putney, J. W., Jr. (1990) *Cell Calcium 11*, 611−624.
27. McHale, M., Coldwell, M. C., Herrity, N., Boyfield, I., Winn, F. M., Ball, S., Cook, T., Robinson, J. H., and Gloger, I. S. (1994) *FEBS Lett. 345*, 147−150.
28. Chio, C. L., Drong, R. F., Riley, D. T., Gill, G. S., Slightom, J. L., and Huff, R. M. (1994) *J. Biol. Chem. 269*, 11813−11819.
29. Asghari, V., Sanyal, S., Buchwaldt, S., Paterson, A., Jovanovic, V., and Van Tol, H. H. (1995) *J. Neurochem. 65*, 1157−1165.
30. Lanau, F., Zenner, M. T., Civelli, O., and Hartman, D. S. (1997) *J. Neurochem. 68*, 804−812.
31. Putney, J. W., Jr., and Bird, G. S. (1993) *Endocr. Rev. 14*, 610−631.
32. Penner, R., and Neher, E. (1988) *J. Exp. Biol. 139*, 329−345.
33. Patel, Y. C., and Srikant, C. B. (1994) *Endocrinology 135*, 2814−2817.
34. Mei, Y. A., Griffon, N., Buquet, C., Martres, M. P., Vaudry, H., Schwartz, J. C., Sokoloff, P., and Cazin, L. (1995) *Neuroscience 68*, 107−116.
35. Akbar, M., Okajima, F., Tomura, H., Majid, M. A., Yamada, Y., Seino, S., and Kondo, Y. (1994) *FEBS Lett. 348*, 192−196.

36. Tomura, H., Okajima, F., Akbar, M., Abdul Majid, M., Sho, K., and Kondo, Y. (1994) *Biochem. Biophys. Res. Commun. 200*, 986−992.
37. Kubota, A., Yamada, Y., Kagimoto, S., Yasuda, K., Someya, Y., Ihara, Y., Okamoto, Y., Kozasa, T., Seino, S., and Seino, Y. (1994) *Biochem. Biophys. Res. Commun. 204*, 176−186.
38. Murthy, K. S., Coy, D. H., and Makhlouf, G. M. (1996) *J. Biol. Chem. 271*, 23458−23463.
39. Chen, L., Fitzpatrick, V. D., Vandlen, R. L., and Tashjian, A. H., Jr. (1997) *J. Biol. Chem. 272*, 18666−18672.
40. Vallar, L., Muca, C., Magni, M., Albert, P., Bunzow, J., Meldolesi, J., and Civelli, O. (1990) *J. Biol. Chem. 265*, 10320−10326.
41. Senogles, S. E. (1994) *J. Biol. Chem. 269*, 23120−23127.
42. Clawges, H. M., Depree, K. M., Parker, E. M., and Graber, S. G. (1997) *Biochemistry 36*, 12930−12938.
43. Senogles, S. E., Spiegel, A. M., Padrell, E., Iyengar, R., and Caron, M. G. (1990) *J. Biol. Chem. 265*, 4507−4514.
44. Tang, L., Todd, R. D., Heller, A., and O'Malley, K. L. (1994) *J. Pharmacol. Exp. Ther. 268*, 495−502.
45. O'Hara, C. M., Tang, L., Taussig, R., Todd, R. D., and O'Malley, K. L. (1996) *J. Pharmacol. Exp. Ther. 278*, 354−360.
46. Yamaguchi, I., Harmon, S. K., Todd, R. D., and O'Malley, K. L. (1997) *J. Biol. Chem. 272*, 16599−16602.

BI992354C